Article

Not peer-reviewed version

Insights into the Oxydifficidin's Mechanism of Action

Alisa P. Chernyshova , Valeriya I. Marina , Andrey G. Tereshchenkov , Vladislava E. Sagitova , Maksim A. Kryakvin , Nikolai D. Dagaev , Eugenia G. Yurchenko , Ksenia A. Arzamazova , Elena B. Guglya , Olga A. Belozerova , Sergey I. Kovalchuk , Margarita N. Baranova , Arsen M. Kudzhaev , Anton E. Shikov , Maria N. Romanenko , Vladimir K. Chebotar , Maria S. Gancheva , Maria E. Baganova , Mikhail V. Biryukov , Tatiana V. Panova , Maria G. Khrenova , Vadim N. Tashlitsky , Natalia V. Sumbatyan , Yulia V. Zakalyukina , Kirill S. Antonets , Anton A. Nizhnikov , Stanislav S. Terekhov , Maria I. Zvereva , Olga A. Dontsova , Petr V. Sergiev , Vera A. Alferova , Dmitrii A. Lukianov *

Posted Date: 22 September 2025

doi: 10.20944/preprints202509.1868.v1

Keywords: oxydifficidin; antibiotics; antimicrobial activity; translation; *Bacillus*

Article

Insights into the Oxydifficidin's Mechanism of Action

Alisa P. Chernyshova [1,2,3], Valeriya I. Marina [2], Andrey G. Tereshchenkov [4], Vladislava E. Sagitova [1], Maksim A. Kryakvin [1], Nikolai D. Dagaev [2,5], Eugeniya G. Yurchenko [6], Kseniya A. Arzamazova [6], Elena B. Guglya [3], Olga A. Belozerova [3], Sergey I. Kovalchuk [3], Margarita N. Baranova [3], Arsen M. Kudzhaev [3], Anton E. Shikov [7,8], Maria N. Romanenko [7,8], Vladimir K. Chebotar [8], Maria S. Gancheva [7,8], Maria E. Baganova [8], Mikhail V. Biryukov [9,10], Tatiana V. Panova[2], Maria G. Khrenova[2,11], Vadim N. Tashlitsky [2,4], Natalia V. Sumbatyan [2], Yulia V. Zakalyukina [1,12], Kirill S. Antonets [7,8], Anton A. Nizhnikov [7,8], Stanislav S. Terekhov [3], Maria I. Zvereva[2], Olga A. Dontsova[1,2,3], Petr V. Sergiev [1,2], Vera A. Alferova [3,4] and Dmitrii A. Lukianov* [1,2].

[1] Center for Molecular and Cellular Biology, 121205 Moscow, Russia
[2] Department of Chemistry, Lomonosov Moscow State University, Moscow 199992, Russia
[3] Shemyakin-Ovchinnikov Institute of Bioorganic Chemistry, Miklukho-Maklaya 16/10, Moscow 117997, Russia
[4] A.N. Belozersky Institute of Physico-Chemical Biology, Lomonosov Moscow State University, 1/40 Leninskie Gory, Moscow 119992 Russia
[5] Faculty of Bioengineering and Bioinformatics, Lomonosov Moscow State University, Moscow 199992, Russia
[6] North Caucasian Federal Scientific Center of Horticulture, Viticulture, Winemaking, Krasnodar 350901, Russia
[7] Biological Faculty, St. Petersburg State University, 199034 St. Petersburg, Russia;
[8] All- Russia Research Institute for Agricultural Microbiology, 196608 St. Petersburg;
[9] Department of Biology, Lomonosov Moscow State University, 119991 Moscow, Russia
[10] Scientific Center for Translational Medicine, Sirius University of Science and Technology, 354340 Sochi, Russia
[11] Bach Institute of Biochemistry, Federal Research Centre "Fundamentals of Biotechnology" of the Russian Academy of Sciences, 119071 Moscow, Russia
[12] Soil Science Faculty, Lomonosov Moscow State University, Moscow 119991, Russia
* Correspondence: Dmitrii A. Lukianov lukianovda@my.msu.ru

Abstract

Oxydifficidin is a natural polyketide antibiotic that is a long-known ribosome-targeting antibiotic that inhibits protein synthesis. In this paper, we describe *Bacillus velezensis* strain EV17 and compare its complete genome sequence with that of the previously characterized strain K-3618 and the difficidin biosynthetic gene cluster (BGC) combined with mass spectrometry, to elucidate the production of oxydifficidin by these strains. Isolated oxydifficidin was determined to increase generalized inhibition of translation at each step of protein biosynthesis using toeprinting and small fluorescent peptide assays. In previous studies, it has been demonstrated that oxydifficidin targets L7/L12 protein. Although spontaneous mutations in ribosomal protein L7/L12, located relatively close to the thiostrepton binding site on uL11, confer resistance to oxydifficidin, our data show that oxydifficidin binding does not interfere with thiostrepton, thereby refining previous findings about its putative ribosomal target. We show that this compound does not affect eukaryotic translation and has no toxic effect on eukaryotic cells. These facts are important to further investigate its potential as a bioprotectant against phytopathogens or even as a therapeutic activity.

 doi:10.20944/preprints202509.1868.v1

Keywords: oxydifficidin; antibiotics; antimicrobial activity; translation; *Bacillus*

1. Introduction

The global rise in antibiotic resistance presents a critical threat to public health, necessitating the discovery and development of novel antimicrobial agents [1]. In the search for novel antimicrobials, the scientific community has traditionally focused on the discovery of entirely new chemical scaffolds. However, this approach is increasingly constrained by the limited success rate of high-throughput screens and the rediscovery of known compounds [2]. In contrast, an often-overlooked strategy involves the systematic re-evaluation of previously discovered antibiotics that were either shelved due to suboptimal pharmacological profiles, narrow spectra of activity, or incomplete understanding of their mechanisms of action [3]. With modern analytical tools—such as high-resolution mass spectrometry, various methods for assessing the mechanism of action, and genome-wide fitness profiling—it is now possible to reassess these molecules with far greater precision and depth [4].

Bacteria represent a major source of novel antibiotic compounds from natural environments. Among them, filamentous actinomycetes produce up to 64% of identified classes of natural antibiotics, and the rest are found in other bacteria and fungi [5–7]. Nevertheless, gram-positive bacteria belonging to Firmicutes, in particular, *Bacillaceae* species, are also considered as important producers of structurally diverse classes of natural antibiotics including antibiotic polypeptides [8–10], polyketides [11,12], and lipopeptides [13–16].

Polyketides are structurally diverse natural metabolites exhibiting a wide range of biological activities, notably antimicrobial effects [13,17,18]. Many polyketide antibiotics are produced by soil bacteria, including *Bacillaceae* species, and contribute to the biocontrol of plant pathogens and potentially have agricultural application [11,13]. However, some polyketide antibiotics, such as oxydifficidin, were historically overlooked due to their low stability. Nevertheless, they remain valuable for providing insights into antibacterial mechanisms of action, motivating renewed investigation.

In this article, we examine the natural polyketide antibiotic oxydifficidin (Oxy), which inhibits protein synthesis by an as-yet-unknown mechanism. We investigate specific steps in translation and the associated binding sites to elucidate Oxy's mode of action.

2. Results and Discussion

2.1. Classification of strains EV17 and K-3618

2.1.1. Genome Sequencing and Annotation

We have sequenced and assembled the genome of the oxydifficidin-producing strain EV17. The mean coverage of Illumina reads was 644. The assembly of the strain resulted in one circular contig – a full chromosome (1 contig), with a total genome length (equal to N50) of 3,978,750 base pairs (bp). The assembly exhibited a GC-content of 46.53%. CheckM [19] analysis of assembly quality revealed a nearly complete genome (98.82%) with no detectable contamination (0%).

Genome sequencing and annotation of the strain K-3618 were reported in our recent preprint [20]. Comparative testing of our *B. velezensis* strains EV17 and K-3618 was conducted against previously published strains FZB42 and NRRL B-41580^{T}. According to our comparison of genes *amyE* and clusters of several antibiotics (Bacillaene, Fengycin, Macrolactin, Difficidin), we can see that the identity of the strain is 96% or higher, which proves that it is the same strain (Table 1, Table S1) [21].

Table 1. Comparative analysis of genomes of *B. velezensis* strains.

 doi:10.20944/preprints202509.1868.v1

	EV17	FZB42 [22]	NRRL B-41580^T [23]	K-3618
General features				
DNA GC content	46.5%	46.5%	46.3%	46.4%
Genome size (bp)	3,978,967	3,918,589	4,034,335	3,864,632
Protein CDS	3829	3693	3790	3734
Extracellular carbohydrate degrading enzymes				
Amylase AmyE	98.23%	100%	96.41%	100%
Non-ribosomal synthesis of lipopeptides and polyketide				
Bacillaene (GenBank ID: AJ634060.2)	98.68%	100%	98.07%	100%
Fengycin (AJ576102.1[1])	98.36%	100%	97.92%	Low coverage
Macrolactin H (AJ634061.2)	98.83%	100%	98.2%	100%
Difficidin (AJ634062.2)	98.64%	100%	98.06%	100%

[1] *B. velezensis* partial genome, strain FZB42, containing *fenE* gene responsible for fengycin synthesis.

Overall, genome sequencing of endophytic and rhizospheric strains EV17 and K-3618 revealed that it belongs to the species *B. velezensis*, a species often closely associated with plants, and well known for promoting plant growth and biocontrol [24]. As strain EV17 as K-3618 are most related to the commercially used *B. velezensis* FZB24 (TAEGRO®), previously known as the type-strain of *B. amyloliquefaciens* subsp. *plantarum* [22].

2.1.2. Whole Genome Phylogeny

The phylogenetic analysis based on whole-genome sequences showed that both strains EV17 and K-3618 formed a well-supported clade with strains belonging to *B. velezensis* with 81% bootstrap value (Figure 1): in addition to the type representative of *B. velezensis*, NRRL B-41580^T, described in 2005 [23], this clade includes strains KACC 13105, originally described as *Bacillus methylotrophicus* sp. nov. [25], strain FZB42 known since 2011 as *Bacillus amyloliquefaciens* subsp. *plantarum* [22], but later reclassified as *B. velezensis*, and two strains, "Bacillus oryzicola" and "Bacillus ayatagriensis", which now have unconfirmed nomenclatural status.

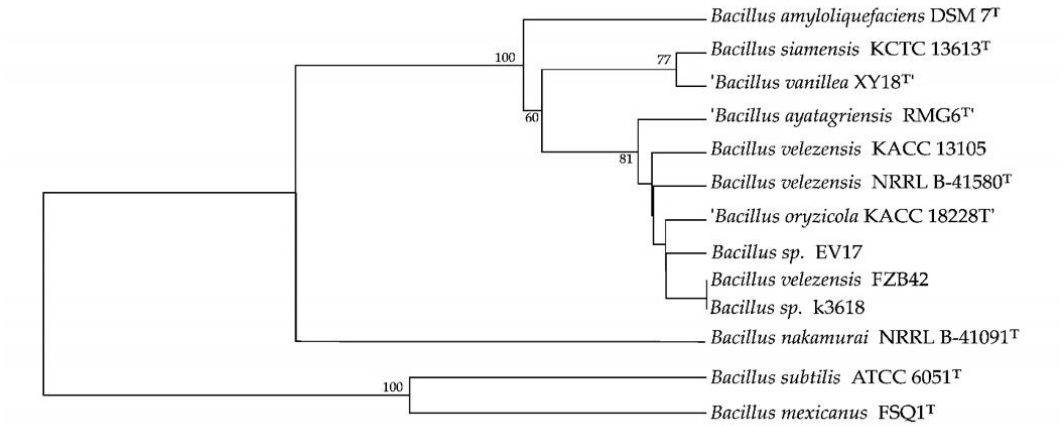

Figure 1. Tree inferred with FastME 2.1.6.1 [26] from GBDP distances calculated from genome sequences. The branch lengths are scaled in terms of GBDP distance formula d5. The numbers above branches are GBDP pseudo-bootstrap support values > 60 % from 100 replications, with an average branch support of 56.5 %. The tree was

 doi:10.20944/preprints202509.1868.v1

rooted at the midpoint [27]. The names of species with unconfirmed nomenclatural status are given in quotation marks.

To confirm the taxonomic identification, we calculated average nucleotide identity (ANIb) between EV17 and K-3618 and closest genomes from *B. velezensis* clade. This revealed that EV17 and K-3618 share more than 98.0% ANI with the genomes that are currently classified as *B. velezensis* (Table 1).

Digital DNA-DNA hybridizations (DDH) indicated that DNA–DNA relatedness between EV17 and K-3618, from one hand, and type strain *B. velezensis* NRRL B-41580^T, from other, are 85.8% (Table 2), which is more than the cut-off point of 70% recommended for the assignment of bacteria strains to the same genomic species [28].

Therefore, the ANIb and dDDH values supported the conclusion that strains EV17 and K-3618 should be considered as representatives of *B. velezensis*.

Table 2. The characteristic and comparison of the whole genome of EV17 and K-3618 with their closest *B. velezensis* strains.

Strain	dDDH for strains		ANIb for strains		Diff. DNA GC content		Accession no.
	EV17	K-3618	EV17	K-3618	EV17	K-3618	
EV17	--	90.3	--	98.82	--	0.13	PRJNA1320960
K-3618	90.3%	--	98.82%	--	0.13%	--	GCA_050472105.1
B. velezensis FZB42	90.4%	100%	98.77%	99.99%	0.05%	0.08%	GCA_000015785
B. velezensis NRRL B-41580^T	85.8%	85.8%	98.19%	98.25%	0.21%	0.08%	GCA_001461825
B. velezensis KACC 13105	84.9%	85.1%	98.13%	98.16%	0.1%	0.03%	GCA_000960265

2.2. Oxydifficidin Isolation

B. velezensis strains coded as EV17 and K-3618 were cultivated in 750 mL Erlenmeyer flasks with 250 mL of liquid Organic medium 79 (g/L), for the synthesis of antibacterial substances using E. coli ΔtolC pDualrep2 and E. coli lptD^{mut} pDualrep2.1 reporter strains [29]. Since cultural broth demonstrated significant antibacterial activity (inhibition zone diameter 13 mm), we carried out primary purification on LPS-500-H sorbent. Both cultural broth and elution with 50%-75% aqueous acetonitrile demonstrated strong induction of the reporter protein Katushka2S (Figure S1), similar to that observed with erythromycin, indicating that antibacterial compound produced by strains EV17 and K-3618 may negatively affect protein synthesis in bacterial cells. The most active fraction (eluted at about 75% ACN) was further analyzed by HPLC using Gemini NX C18 column with isocratic elution at 40% of MeCN in 10 mM NH4OAc (Figure S2). HPLC fractions were tested for activity, and the fraction containing pure active substance was isolated and then analyzed by LC-MS.

2.3. Identification of Antibacterial Compound Oxydifficidin Produced by Strains EV17 and K-3618

Taking into account the plausible inhibition of protein synthesis by the active component, as well as the presence of genes demonstrating high similarity to difficidin BGC (BGC0000176), detected by the AntiSMASH in the whole-genome of EV17 and K-3618 (Figure 2A), we identified active compound by HR-LCMS. Analysis of the active fraction using HR-LCMS revealed an ion with *m/z* 583.2828, corresponding to the $[M+Na]^+$ adduct of oxydifficidin ($C_{31}H_{45}O_7P$), which is an oxidized form of difficidin [30], known to be produced by organisms, encoding the *dif* cluster [31,32]. In the same spectrum, characteristic fragment ions were observed at *m/z* 480.34 (M – phosphate), *m/z* 463.32

 doi:10.20944/preprints202509.1868.v1

(M – phosphate – H_2O) and *m/z* 445.31 (M – phosphate – $2H_2O$), supporting the structural assignment (Figure 2B). Complementary HR-LCMS in negative mode revealed an ion with *m/z* 559.2708, which also confirmed the identification of oxydifficidin. Additional comparison of MS data (Figure S3, S4), UV spectra (Figure S2) and the proposed mechanism of action against bacterial translation with previously published data [30,31] corroborated the production of oxydifficidin by the studied strains.

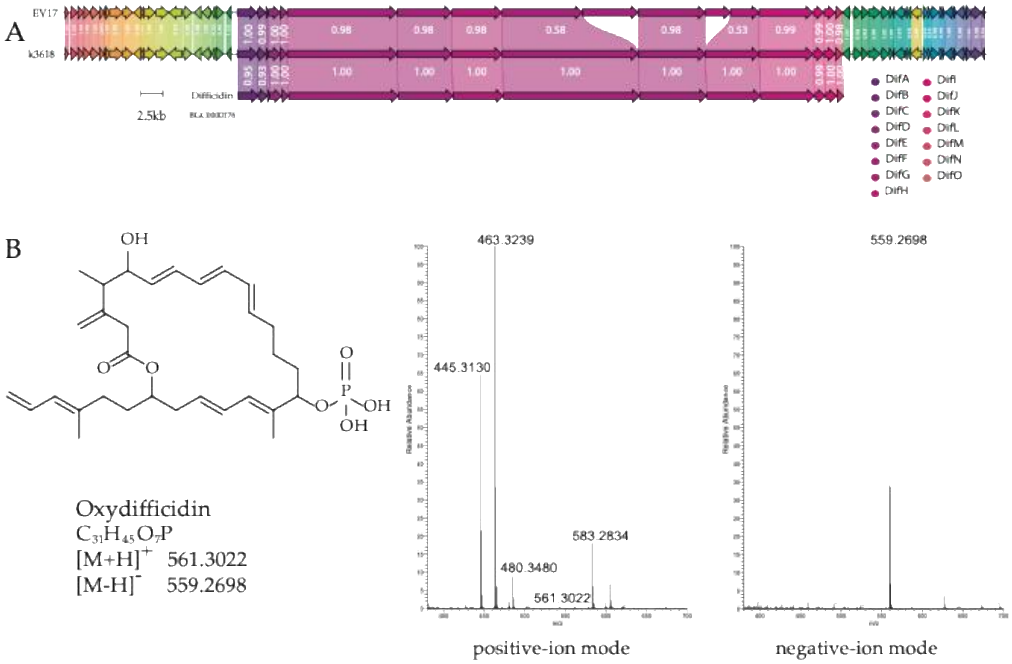

Figure 2. (A) Analysis of bioactive metabolites from the strains EV17 and K-3618: a comparison of difficidin BGC (BGC0000176) with regions 3 in the EV17 and K-3618 complete genome sequence, generated using clinker tool [33]. All three BGCs harbor a highly similar biosynthetic gene cluster; additionally, EV17 and K-3618 genomes exhibit extended conserved synteny of flanking regions (both upstream and downstream of the cluster), indicating a shared genomic context beyond the core locus. Homologous genes are highlighted with colors, and labels indicate identity of the genes. (B) Structure and HR-LCMS spectra of the isolated oxydifficidin.

2.4. Biological Activity of Oxydifficidin

2.4.1. Oxydifficidin Exhibits Antibacterial Activity

After isolation and purification of the active compound - oxydifficidin, the agar plate test was repeated (Figure 3). We employed a reporter test strain that expresses fluorescent proteins in response to sublethal antibiotic concentrations, depending on their mechanism of action. Activation of the SOS response induced TurboRFP expression, while translation inhibition, characterized by ribosome stalling on mRNA, triggered Katushka2S expression. In both cases, strong induction of the reporter is visualized, similar to that observed with erythromycin, suggesting that oxydifficidin may have negative effect on protein biosynthesis in bacterial cells, as previously shown [30].

 doi:10.20944/preprints202509.1868.v1

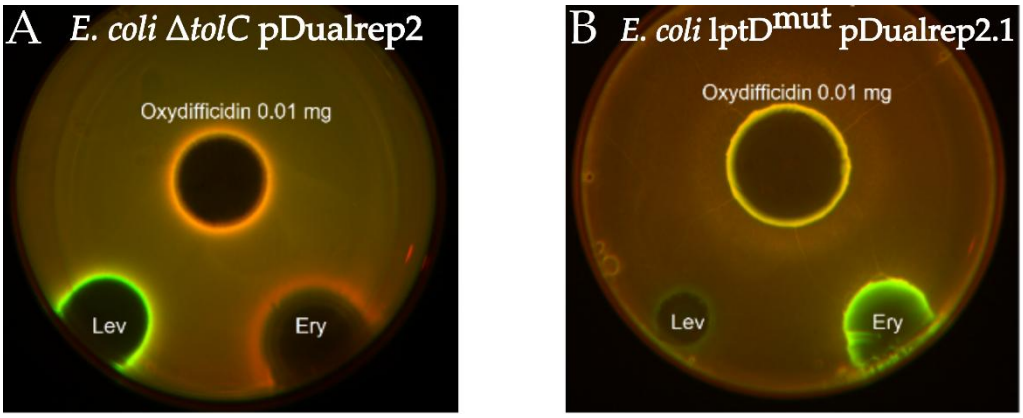

Figure 3. Oxydifficidin inhibits protein synthesis in bacteria cells. Agar plates coated with **(A)** *E. coli ΔtolC* pDualrep2 [34] and **(B)** *E. coli lptD*^{mut} pDualrep2.1 reporter strains and spotted with oxydifficidin (0.01 mg) along with erythromycin (Ery) (5 mg/ml) and levofloxacin (Lev) (25 mg/ml) [29]. The plates were scanned in Cy3 (for TurboRFP) and Cy5 (for Katushka2S) channels, shown as green and red pseudocolor, respectively.

For subsequent experiments, we determined the minimum inhibitory concentration (MIC) of oxydifficidin. An overnight culture of the *E. coli* BW25113 lptD^{mut} strain [35] was diluted to an optical density (OD600) of 0.05–0.1, and oxydifficidin, along with the control antibiotic erythromycin, was added using a standard two-fold serial dilution method. Cultures were incubated overnight at 37°C with shaking. MIC, defined as the lowest antibiotic concentration that completely inhibited visible bacterial growth, was determined to be 20 μg/mL (36 μM) for oxydifficidin against the *E. coli* BW25113 lptD^{mut} strain.

2.4.2. Oxydifficidin Inhibits Prokaryotic In Vitro Translation

To directly evaluate the ability of Oxy to inhibit protein synthesis, we employed in vitro translation system: a reconstituted system of purified components (PURExpress® In Vitro Protein Synthesis Kit, NEB), using reporter system based on luciferase mRNA. In both systems, translation efficiency was monitored by measuring luciferase activity, which depends on the enzymatic conversion of d-luciferin to oxyluciferin, with chemiluminescence recorded on a VICTOR X5 Light Plate Reader. Oxy was titrated over a concentration range spanning sub-MIC to supra-MIC levels as was previously established for *E. coli* BW25113 lptD^{mut} strain (Figure 4B), with complete inhibition of protein synthesis observed at 2 μg/mL (3.6 μM). These results confirm that Oxy is a potent inhibitor of bacterial protein synthesis.

Previous publications have assessed in vitro inhibition of translation by difficidin. They have shown that 2 μg/mL (3.6 μM) completely inhibits the incorporation of radioactive amino acids in nascent peptides [30]. These data align with our findings for the difficidin derivative oxydifficidin, which likewise fully inhibits translation at 3.6 μM.

2.4.3. Oxydifficidin Cause Generalized Inhibition of Translation

To investigate the mechanism of action of Oxy during translation, we performed a toeprinting assay to monitor ribosome positioning on the *ErmDL* mRNA using reverse transcription (Figure 4A). Reactions were carried out in the absence of antibiotic as well as in the presence of Oxy and the control antibiotic thiostrepton (Ths). As expected, in the absence of antibiotic, multiple bands were observed, corresponding to translating ribosomes distributed across the open reading frame. In contrast, the addition of Ths resulted in the appearance of a strong band corresponding to inhibition at the initiation step [36]. By comparison, Oxy did not produce defined stalling sites but instead caused generalized inhibition, with stops distributed across multiple codons. This suggests that oxydifficidin is lacking detectable context specificity and is likely capable of undergoing multiple rounds of binding and dissociation from the ribosome during elongation.

 doi:10.20944/preprints202509.1868.v1

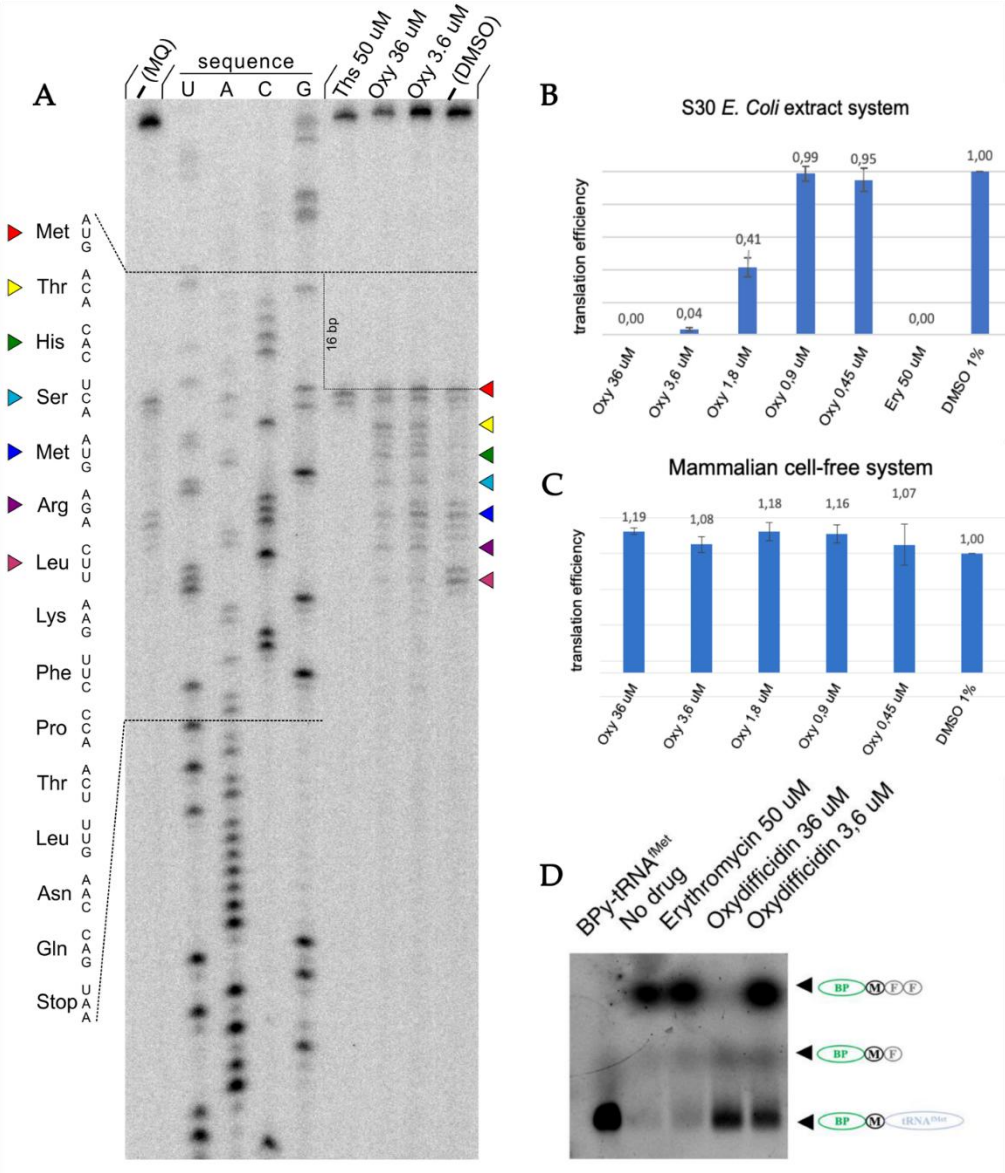

Figure 4. Oxydifficidin inhibits prokaryotic translation, but not eukaryotic.

(A) Oxy causes non-specific pauses in translation distributed across multiple codons. Toeprinting assay of *ErmDL* template in the presence or absence (-) of Oxy at various concentrations and control antibiotic thiostrepton (Ths). Ths inhibits initiation (red arrow), while Oxy did not cause ribosome stalling at specific mRNA sites but instead caused non-specific pauses distributed across nearly every codon. Negative controls (DMSO, MQ - without addition of antibiotics) translate the whole length of mRNA. (B) In vitro translation in the *E. coli* S30 extract system. Oxydifficidin inhibits prokaryotic translation in a concentration-dependent manner. Positive control - erythromycin (50 μM), negative control - 1% DMSO. The graph represents means of three independent replicates; error bars indicate ±SD. (C) In vitro translation in the mammalian cell-free HEK293 lysate system. The graph represents means of three independent replicates; error bars indicate ±SD. (D) The products of MF2-coding mRNA in vitro translation in the presence of BPY-Met-tRNA^{fMet} and antibiotics indicated above the lanes: oxydifficidin 3.6 μM and 36 μM concentrations, erythromycin 50 μM along with control BODIPY-Met-tRNA^{fMet} itself (BPy) and sample without antibiotics as a negative control (DMSO 1%). BPy is marked with a green oval— BODIPY label; dark grey circle—methionine; light grey circle—phenylalanine residue; blue oval—tRNA^{fMet}.

2.4.4. Oxydifficidin Practically Does Not Inhibit Initiation Step of Bacterial Translation

 doi:10.20944/preprints202509.1868.v1

To clarify the mechanism of action of oxydifficidin in more detail, an experiment was conducted using the MF2 template encoding a short peptide consisting of three amino acids—methionine and two phenylalanines [37]. Briefly, each translation product is labeled by the fluorescent N-terminal BODIPY (BPy) group introduced via initiator BPy- Met-tRNA^{fMet}. This system allows visualization of disruptions at various stages of translation due to the unusual mobility of BODIPY-labeled products in RNA-urea PAGE.

We have shown that at high concentrations (36 μM), oxydifficidin completely suppresses the synthesis of the full-length short peptide, although slight band of dipeptide product is seen (Figure 4D). Therefore, we can assume that oxydifficidin affects peptidyl-transferase reaction or translocation step of translation.

According to the toeprinting and BPy assays, oxydifficidin may also partially affect initiation. To directly test whether translation initiation is impacted, we employed a template encoding only a single amino acid, methionine. Since released methionine is detected, we can conclude that initiation is unaffected by oxydifficidin (Figure S5).

2.4.5. Competition for the Thiostrepton Binding Site

Recently, two spontaneous mutations (K84E and R76C) in the L7/L12 protein were shown to confer resistance to Oxy [38]. L7/L12 is a multi-copy component of the L10/L7 stalk of the 50S subunit: its flexible C-terminal domains recruit and stabilize the binding of ribosome-associated GTPases (e.g., EF-G, IF2, RF3), promote their activation and stimulate GTP hydrolysis, thereby facilitating initiation, elongation and termination of translation [39,40]. Thiostrepton (Figure S6A) binds to ribosomal protein uL11 in the GTPase-associated center; its binding site is located in close proximity to the L10/L7 stalk and the L7/L12 protein (Figure S6B) [41]. We therefore investigated whether the binding sites of Oxy and Ths overlap on the ribosome.

To address this, we synthesized a fluorescent thiostrepton derivative, Ths-FITC (Figure S6A), in which a fluorescein tag was attached to a truncated thiostrepton analog (thuncThs) via the peptide linker βASGSGC to improve solubility. Conjugation of the FITC-βASGSGC peptide to the dehydroalanine residue of thuncThs was performed by sulfa–Michael addition following a published procedure [42].

The resulting fluorescent derivative Ths-FITC bound to *E. coli* 70S ribosomes with high affinity (Figure S6C), showing an apparent dissociation constant (K_D) in the subnanomolar range. In a competitive binding assay, we evaluated Oxy's ability to displace Ths-FITC from its ribosomal binding site (Figure 5). Unlike Ths and thuncThs, which showed strong ribosome binding ($K_D \approx 0.26$ and 0.21 nM, respectively — consistent with literature values for binding to a reconstituted complex of protein uL11 and 23S rRNA [42]), Oxy did not appreciably displace Ths-FITC.

Thus, oxydifficidin likely binds to a different site or even target, distinct from the Ths binding site that involves uL11 and helices H43/H44 of 23S rRNA.

 doi:10.20944/preprints202509.1868.v1

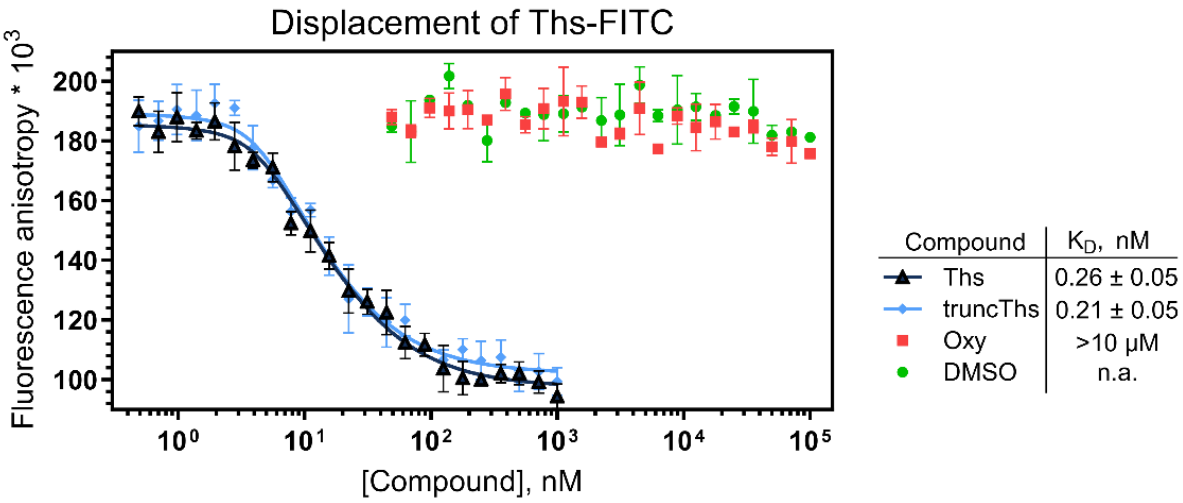

Figure 5. Oxydifficidin does not compete for the thiostrepton binding site. A competitive binding assay measuring the ability of Ths, its truncated analog (truncThs), and Oxy to compete for the thiostrepton binding site on *E. coli* 70S ribosomes, using fluorescence anisotropy of fluorescently labeled truncated thiostrepton (Ths-FITC). A 5% DMSO solution was used as a control. Data represent means of four independent replicates; error bars indicate ±SD. The apparent dissociation constants (K_D) with CI ($\alpha = 0.05$) are shown. n.a. – not applicable.

2.4.6. Oxydifficidin Does Not Affect Eukaryotic Translation or Cell Viability

Since oxydifficidin effectively inhibits prokaryotic translation, it was decided to test whether this antibiotic would inhibit translation in a cell-free system based on mammalian cell lysate HEK293. As for prokaryotic systems, different concentrations of Oxy were used. Oxydifficidin has been shown to have no effect on eukaryotic translation (Figure 4C).

Oxydifficidin and difficidin were not previously assessed for inhibiting in vitro translation in the eukaryotic system. In this study, we showed that Oxy does not affect eukaryotic translation in a wide range of concentrations, ending with a quite large 36 μM.

The cytotoxicity of Oxy was assessed for the immortalized human embryonic kidney cell line HEK293T. The MTT assay revealed that the IC50 for Oxy was higher than 250 mg/L (≈ 450 μM).

Overall, *B. velezensis* is a promising bacterial species for plant protection [13,43] producing a wide spectrum of natural antibiotics and serving as plant growth-promoting bacteria [44–46]. Some strains of this species exhibit broad-spectrum antibacterial and antifungal activities, produce siderophores such as bacillibactin (confirmed in their genomes), and form biofilms with remarkable protective properties, making them particularly well-suited for sustainable agricultural applications [43,47,48]. Here we show that two *B. velezensis* strains, EV17 and K-3618, produce a bioactive compound that was identified as oxydifficidin. We demonstrate that despite oxydifficidin inhibiting bacterial protein synthesis, it does not affect eukaryotic translation and does not cause detectable toxicity to eukaryotic cells. This selective activity supports an idea that oxydifficidin can be safely used as a protective agent against bacterial phytopathogens [49,50], offering a promising alternative to chemical pesticides.

3. Materials and Methods

3.1. Producents' Characterization

3.1.1. Collection, Isolation and Preservation

The oxydifficidin-producing strain EV17 was isolated from grapevine *Vitis L.* obtained via crossing European and American grape varieties *V. vinifera* × (*V. vinifera* + *V. labrusca* +*V. riparia* +*V. rupestris* + *V. berlandieri* + *V. aestivalis* + *V. cinerea*). The vineyard of 'Moldova', 26 years old, was located

 doi:10.20944/preprints202509.1868.v1

on the coast of the Azov Sea (Temryuk district, Krasnodarsky area). The variety belongs to the Euro-American genetic group and is an interspecific hybrid that is suitable for table use. This sort has a complex resistance to the main diseases of grapes – oidium (*Uncinula necator*), mildew (*Plasmopara viticola*), and gray rot (*Botrytis cinerea*).

The grapevine tissues (one-year shoots and mature stems) were collected in triple repetitions on July 28, 2021 and immediately transported to the laboratory. The samples (2.0 g) were surface-sterilized with 70% ethanol (1 min), then exposed in 5% NaClO (1 min) and trice rinsed with sterile distilled water. After drying at room temperature under aseptic conditions they were crushed in a sterile mortar with saline solution (10 ml of solution per 1 g of substrate) and 0.1 mL aliquots were transferred to MPA plates. After 3 days incubation at 28°C, the grown endophytic bacteria were sampled and carefully transferred to a new sterile Petri dish for repeated cultivation. The long-term storage of the isolates was carried out as cell suspensions in LB media [51] with glycerol (20 %, v/v) at −80°C.

Another oxydifficidin-producing strain *B. velezensis* K-3618 was obtained from the collection of the All-Russian Research Institute of Agricultural Microbiology, ID RCAM 07246. Strain K-3618, an endophytic microorganism isolated from potato tubers of the Charoit variety, exhibits cellulolytic, amylolytic, and weak nitrogen-fixing activity.

3.1.2. Cultivation

To obtain a sufficient amount of the active compound for detailed bioactivity studies, strain EV17 was cultured in four 750 mL Erlenmeyer flasks with 250 mL of liquid Organic medium 79 (g/L: glucose 10, peptone 10, yeast extract 2, hydrolysate casein 2, NaCl 6; pH 7.0) at 28°C with shaking (200 rpm) for 3 days. Culture liquids were separated from biomass by centrifugation at 20,000× g for 20 min (Centrifuge 5810 R, Rotor FA-45-6-30, Eppendorf, Hamburg, Germany)

Strain K-3618 was initially grown on agar at 37°C. A portion of the culture was transferred to a 750 mL Erlenmeyer flask containing 50 mL of 2YT medium (g/L: tryptone 16, yeast extract 10, NaCl 5; pH 7.0) and incubated at 28°C for 24 h with shaking at 150 rpm on an Innova 40 thermostat shaker (New Brunswick Scientific, Edison, NJ, USA). The resulting culture was used as a 3% (v/v) inoculum to seed a second-generation culture in 150 mL of the same medium, which was cultivated under identical conditions.

3.1.3. Phenotypic Characterization

Cultural characteristics of EV17 and K-3618 were determined after incubation for 3 days at 28°C on Organic media 79 and LB agar. Gram staining of cells was carried out using a Gram-reagent kit (OOO NICF, Russia). Cell morphology was examined under light microscope (magnification ×1500) with oil immersion. Enzymes and carbon source utilization were investigated using paper discs to differentiate bacteria (Microgen, Russia).

3.1.4. Genome Sequencing and Annotation

The genomic data for the strain K-3618 were taken from the previous research [20]. To obtain a high-quality assembly of the strain EV17, both Il-lumina and Oxford Nanopore platforms, were employed. The LumiPure kit (Lumiprobe, USA) was used to isolate genomic DNA of EV17. A paired-end DNA library was prepared using the NEBNextUltra II DNA Library Prep Kit (Illumina) and NEBNext Multiplex Oligos for Illumina (96 Unique Dual Index Primer Pairs) according to manufacturer instructions. Whole-genome sequencing was carried out by NovaSeq6000 sequencing platform (Illumina) with 2 × 250 bp read length using NovaSeq 6000 SP Reagent Kit v1.5 (500 cycles) according to the manufacturer's protocol. Long genomic DNA reads were obtained by means of Oxford Nanopore Technologies (Oxford, UK). Fraction of high-molecular weight DNA was used for library preparation using the ONT Native Barcoding Kit V14 (SQK-NBD114) according to manufacturer instructions. Further sequencing was performed using R10.4.1 PromethION Flow Cell

 doi:10.20944/preprints202509.1868.v1

by means of ONT PromethION P2 sequencing platform, according to the manufacturer's protocol (Oxford Nanopore Technologies, Oxford, UK). Nanopore sequencing of genomic DNA was performed using the ligation sequencing protocol SQK-LSK109 (Oxford Nanopore Technologies, Oxford, UK). Sample preparation followed the procedure described in reference [52]. Flow cell loading and library preparation were carried out according to the manufacturer's instructions. The final DNA library was loaded onto an R9.4.1 MinION Mk flow cell (Oxford Nanopore Technologies, UK).

For multiplexed sequencing of several strains in a single run, a barcoding step was introduced prior to adapter ligation using the Native Barcoding Expansion 1–12 kit (EXP-NBD104, Oxford Nanopore Technologies, UK). Barcoding was performed according to the manufacturer's protocol, which parallels the adapter ligation workflow and includes barcode ligation and DNA purification steps. Following barcoding ligation, equimolar DNA samples were pooled for the subsequent adapter ligation step.

Nanopore reads were assembled with Flye (v2.9.5) [53]. Raw Illumina sequencing reads were initially subjected to quality assessment using FastQC (v0.12.1) [54], and subsequent filtering of low-quality and adapter-contaminated reads was performed with fastp (v0.24.1) [55]. To correct sequence errors in genomes assembled with long reads, Illumina reads and Nanopore assembly were used with NextPolish (v1.4.1) [56]. The construction of the phylogenetic tree was carried out using FastME v.2.1.1.6 analysis based on distance algorithms [26].

3.1.5. Genome-Wide Taxonomy Classification

The genome sequence data were uploaded to the Type (Strain) Genome Server (TYGS), a free bioinformatics platform available under https://tygs.dsmz.de, for a whole genome-based taxonomic analysis [28]. Information on nomenclature and synonymy was provided by TYGS's sister database, the List of Prokaryotic names with Standing in No-menclature (LPSN, available at https://lpsn.dsmz.de) [57]. The results were provided by the TYGS on 2025-08-24.

In silico digital DNA: DNA hybridization (DDH) values were calculated by using the GGDC method, with the recommended formula 2, available at the TYGS web service (https://tygs.dsmz.de/, accessed on 24 August, 2025).

Average nucleotide identity analysis with a sequence pairing based on blast+ (ANIb) analyses were carried out using the JSpeciesWS server https://jspecies.ribohost.com/jspeciesws (date of application 24.08.2025) [58]. Those scores were calculated to compare EV17 and K-3618 with their closest type strains with complete genome.

3.2. Purification and Isolation of Bioactive Compound

3.2.1. Solid-Phase Extraction

Bacterial cells were removed from the culture broth by centrifugation at 5000 rpm (Sigma 3-16KL) followed by filtration through a 0.47 μm MCE membrane filter (Millipore). One liter of the clarified supernatant was loaded onto a 30 mL cartridge containing 7 g of LPS-500-H polymer sorbent (divinylbenzene hydrophilic copolymer, pore size 50–1000 Å, 70 μm; Technosorbent, Russia) at a flow rate of 15 mL/min using a peristaltic pump (Masterflex L/S Variable Speed Pump System, Masterflex). Sequential elution was performed with 15 mL portions of water-acetonitrile (MeCN) mixtures containing 0, 10, 35, 50, 75, and 100% MeCN. The biological activity of each fraction was assessed using the reporter *E. coli* lptD^{mut} strain.

3.2.2. HPLC Separation

The most active fraction, eluted at 75% MeCN, was further analyzed by reverse-phase HPLC using a Nexera X2 LC-30A system (Shimadzu) equipped with an SPD-M20A detector. Separation was performed on a Gemini NX C18 column (150 × 10 mm, 5 μm, 110 Å; Phenomenex) with solvent A (10 mM NH_4OAc, pH 5) and solvent B (MeCN). The elution profile consisted of isocratic elution at 40%

 doi:10.20944/preprints202509.1868.v1

solvent B for 15 min, followed by a gradient to 90% MeCN over 17 min and a 3 min column wash; flow rate was 3 mL/min and detection was at 275 nm. Fractions were collected and assayed for activity; the fraction containing the pure active compound was isolated and subjected to LC-MS analysis.

For biological assays, the active compound was purified on a semipreparative Gemini NX C18 column (150 × 20 mm, 10 µm, 110 Å; Phenomenex) using a PuriFlash 5.250 system (Interchim) under the same solvent conditions, with a flow rate of 16 mL/min.

3.3. Identification of Bioactive Compound

3.3.1. Mass-Spectrometry

LC-MS analysis was carried out on an Ultimate 3000 RSLCnano HPLC system connected to an Orbitrap Fusion Lumos mass spectrometer (ThermoFisher Scientific, Waltham, MA, USA) with the loading pump used for analytical flow gradient delivery. Samples were separated on a Gemini NX-C18 3 µm 100 Å column 100*2.1 mm at 200 µL/min flow rate in the linear gradient of acetonitrile in water with the addition of 10 mM ammonium formate and 0.1% formic acid. UV data were collected at 220 and 280 nm. MS1 and MS2 spectra were recorded at 30K and 15K resolution, respectively, with HCD fragmentation. Raw data were collected and processed on Thermo Xcalibur Qual ver. 4.3.73.11.

3.3.2. Analysis of Antibiotic's Biosynthetic Gene Clusters

Secondary metabolite biosynthetic gene clusters in the complete genome of strains EV17 and K-3618 were identified with the bacterial version of antiSMASH 8.0 [59] (https://antismash.secondarymetabolites.org/ (accessed on 20 August 2025)).

3.4. Biological Activity Testing

3.4.1. Design of Reporter Strain *E. coli* lptD^{mut} pDualrep2.1

E. coli strain SQ110lptD with increased outer membrane permeability was previously developed. We generated a reporter based on this strain, analogous to the previously created *E. coli* ΔtolC pDualRep2 system [34] and designated it as *E. coli* lptD^{mut} pDualrep2.1. Initially, it was anticipated that the *E. coli* BW25113 lptD^{mut} strain could be transformed with the standard AmpR pDualRep2 plasmid [34]. However, the transformed cells exhibited instability under ampicillin selection and survived only at concentrations up to 25 µg/ml. To overcome this limitation, the ampicillin resistance cassette of pDualRep2 was replaced with a kanamycin resistance cassette.

The vector backbone was obtained from pDualRep2, and the kanamycin resistance gene was amplified from the tolC mutant of the KEIO collection [60] using primers pdualrep2_fwd/pdualrep2_rev and KanR_fwd/KanR_rev, respectively (Table S2). PCR products were purified with the Cleanup Mini Kit (Qiagen, Germany) and verified on 1% agarose gel electrophoresis. DNA fragments were assembled using NEBuilder® HiFi DNA Assembly (New England Biolabs) according to the manufacturer's protocol. The assembled products were size-selected on agarose gel and purified with the Cleanup Mini Kit.

For transformation, 1 mL of overnight *E. coli* BW25113 lptD^{mut} culture (OD600 = 2.0) was chilled on ice for 10 min, pelleted by centrifugation at 5000 rpm for 10 min, washed twice with TB buffer (10 mM PIPES, 15 mM $CaCl_2$, 250 mM KCl, 55 mM $MnCl_2$, pH 6.7), and resuspended in 1 mL of TB. Aliquots (100 µl) of competent cells were mixed with 100 ng of pDualRep2-KanR plasmid DNA and incubated on ice for 30 min. Heat shock was performed at 42 °C for 45 s, followed by recovery in 800 µl LB medium at 37 °C for 1 h. Transformants were plated on LB agar containing kanamycin (50 µg/mL) and incubated overnight.

A single colony of *E. coli* BW25113 lptD^{mut} harboring pDualRep2-KanR was inoculated into 50 mL LB medium supplemented with kanamycin and cultured at 37 °C with shaking (100 rpm) for 15

 doi:10.20944/preprints202509.1868.v1

h. The culture was supplemented with sterile glycerol to a final concentration of 25% (v/v), aliquoted (0.5 mL), snap-frozen in liquid nitrogen, and stored at –20 °C.

3.4.2. Reporter Antibacterial Assays on Agar Plates

The two *E. coli* reporter strains: *E. coli* lptD^{mut} pDualrep2.1 and JW5503 *ΔtolC* pDualRep2 were used in this work as previously described [29]. Briefly, the overnight culture of reporter strains was diluted with fresh LB medium to an optical density of 600 nm (OD600) of 0.05-0.1. The culture was transferred to LB agar plates that had 100 mg/mL ampicillin or 50 mg/mL kanamycin applied for JW5503 *ΔtolC* pDualRep2 and *E. coli* lptD^{mut} pDualrep2.1 strains, respectively. On an agar plate with the lawn of one of the reporter strains 10 μg of oxydifficidin was applied along with two control antibiotics: erythromycin (Ery, 5 mg/mL) and levofloxacin (Lev, 25 mg/mL). Plates were incubated at 37 °C overnight and then scanned by ChemiDoc (Bio-Rad) in the modes 'Cy3-blot' for RFP and 'Cy5-blot' for Katushka2S. In the case of SOS-response activation the expression of the *rfp* gene occurred, while the expression of *katushka2S* gene took place in the case of a violation of translation, when the ribosome was stalled on the mRNA template. When scanning, the signal from the RFP protein was displayed in green, and from Katushka2S in red.

3.4.3. MIC Determination

Overnight cultures of tested strains were diluted 1:1000 in LB medium. A two-fold serial dilution was then carried out. The ninety-six-well 2 mL deep-well plates containing *E. coli* KanR culture with and without Oxy, and LB medium as a control, along with erythromycin (Ery), which was used as a control for the experiment, were then incubated overnight at 37 °C with shaking at 200 rpm. Cell growth was measured at 590 nm using a microplate reader (VICTOR X5 Light Plate Reader, PerkinElmer, Waltham, MA, USA).

3.4.4. Bacterial In Vitro Translation Assay

To test the ability of Oxy to inhibit protein synthesis in vitro the PURExpress® In Vitro system (NEB, Ipswich, MA, USA) or *E. coli* S30 Extract System for Linear Templates (Promega) was used. The assembled reactions (5 μL) were supplemented 0.1 mM of d-luciferin (Promega), 0.5 μL of either antibiotic solution or water, and 100 ng of *Fluc* mRNA. All samples were then placed in a 384-well black-wall plate at 37°C. Chemiluminescence was recorded with VICTOR X5 Light Plate Reader. The Fluc mRNA obtained by MEGAscript™ T7 Transcription Kit (ThermoFisher, Carlsbad, CA, USA) from the circular DNA template.

3.4.5. Toeprinting Assay

Toeprinting was carried out according to the protocol described in [35] with minor modifications. Toeprinting reactions were carried out in 5 μL aliquots containing 2 μL of solution A, 1 μL of solution B (PURExpress transcription-translation coupled system (New England Biolabs, USA)), 0.2 μL of RiboLock (ThermoFisher), 0.5 μL of the oxydifficidin (final concentrations 36 and 3,6 μM), 0.5 μL of DNA template ErmDL (100 ng), and 0.5 μL of the 5'-end [^{32}P]-radiolabeled NV1 primer. The reactions were incubated at 37°C for 20 min. Reverse transcription was conducted for 15 min at 37°C using AMV Reverse Transcriptase (New England Biolabs, USA). The reaction was then stopped by adding 1 μL of 10 M NaOH (15 min at 37°C), neutralized by 1 μL 10 N HCl and purified by QIAquick PCR purification kit (Qiagen, Germany). Primer extension products were resolved on 6% polyacrylamide gel containing 19% acrylamide, 1% N,N'-methylenebisacrylamide and 7M urea in TBE buffer. Results were visualized using a Typhoon FLA 9500 Biomolecular Imager (GE Healthcare, US).

The ErmDL template and NV1 primer sequences described in Table S2.

 doi:10.20944/preprints202509.1868.v1

3.4.6. Fluorescently Labeled Short Peptides

Coupled transcription-translation was set up in 5 µl reactions using a PURExpress Δ (aa, tRNA) Kit (NEB) as described previously [37] with minor modifications: 20 ng of MF2 DNA template containing a T7 promoter upstream of the coding sequence, 0.1 µM BPY-Met-tRNA^{fMet}, 0.45 µM fMet-tRNA^{fMet}, 1 µM Phe-tRNA^{Phe}, 100 µM Phe and 1 µL of either antibiotic solution or water were added to each reaction.

To assess the effect of oxydifficidin on translation initiation the experiment was carried out in a system of PURExpress® In Vitro Protein Synthesis Kit using template that encodes one amino acid – methionine (M template). The reactions were divided into two parts: with and without treatment by RNAse A (ThermoFisher) (15 mins incubated on ice). The rest of the protocol was not subject to further changes.

Samples then were preheated for 3 min at 70°C and loaded to a 10% denaturing PAGE (19:1 AA:bisAA; 1× TBE buffer; 7M urea). Gels were scanned by a Typhoon FLA 9500 Biomolecular Imager (GE Healthcare) in the FAM channel with excitation peak (493 nm) and emission peak (517 nm).

3.4.7. Mammalian Cell-Free System

Whole home-made HEK293T cell extracts were used to test compounds in a mammalian in vitro translation system. The reaction was carried out in 10 µl, including 5 µL HEK293T extract, 1 µL 10X translation buffer (20 mM Hepes-KOH pH 7.6, 1 mM DTT, 0.5 mM spermidine-HCl, 0.8 mM $Mg(OAc)_2$, 8 mM creatine phosphate, 1 mM ATP, 0.2 mM GTP, 120 mM KOAc and 25 µM of each amino acid), 2U of RiboLock RNase inhibitor (Thermo Scientific), 0.5 mM d-luciferin (Promega), 1 µL of either antibiotic solution or solvent (water), and 50 ng mRNA (the latter was added to 1 µL of the mixture solution after preliminary incubation of the reaction mixture with the antibiotic for 5 min at 30°C.). After adding the mRNA, the mixtures were transferred to a pre-heated white FB/NB 384 well plate (Grenier no. 781904) and incubated in the VICTOR X5 Multilabel Plate Reader (PerkinElmer, Waltham, MA, USA) at 30 °C with continuous measurement of luciferase activity.

3.4.8. Competition for the Thiostrepton Binding Site

The fluorescence anisotropy method was employed to assess competition at the thiostrepton binding site on the ribosome. 70S ribosomes were purified from *E. coli* MRE600 cells following a published procedure [61]. The fluorescent thiostrepton derivative Ths-FITC was synthesized as previously described [42], with detailed procedures provided in the Supplementary Materials. Binding of Ths-FITC to *E. coli* 70S ribosomes was assessed by incubating 4 nM Ths-FITC with ribosomes (0.1–200 nM) for 2 h at 25 °C in buffer containing 20 mM HEPES-KOH (pH 7.5), 50 mM NH_4Cl, 10 mM $Mg(CH_3COO)_2$, and 0.05% Tween-20. Binding affinities of Ths, its truncated derivative truncThs, and Oxy for the *E. coli* ribosome were determined by a competition-binding assay with Ths-FITC (4 nM) and ribosomes (7.3 nM) in the buffer. Test compounds, initially dissolved in 2,2,2-trifluoroethanol (Ths and truncThs) or DMSO (Oxy), were added to pre-formed complexes at final concentrations ranging from 0.5 nM to 100 µM, ensuring that the concentration of organic solvent did not exceed 5%. The mixtures were then incubated for 4 h at 25 °C. A 5% DMSO solution, corresponding to the highest solvent concentration used in the assay, served as a negative control. Fluorescence anisotropy was measured on a VICTOR X5 Multilabel Plate Reader (PerkinElmer, Waltham, MA, USA) using a 384-well format (excitation wavelength was 485 nm, and the emission wavelength was 535 nm). All measurements were performed in quadruplicate. Apparent dissociation constants were calculated as described [62].

3.4.9. MTT Cytotoxicity Test

The impact of the test compound on cellular metabolic activity, as an indicator of cell viability, was evaluated using MTT reduction assay as described [63]. Investigations were performed solely on

 doi:10.20944/preprints202509.1868.v1

the human embryonic kidney HEK293T cell line. Solvent DMSO served as the reference control compound. Oxy was prepared as DMSO stock solution with a concentration 40 mg/ml.

HEK293T cells were cultured in DMEM/F-12 medium, enriched with 10% FBS and a 1% antibiotic-antimycotic solution (penicillin 50 U/mL, streptomycin 50 μg/mL), under standard conditions (37°C, 5% CO_2). For experimental procedures, cells were plated in triplicate at 2,500 cells/well in 96-well plates and incubated for 24 hours to ensure attachment. Post-attachment, the culture medium was supplemented with serial two-fold dilutions of the compounds; the concentration range for the Oxy was 2–250 mg/L.

The treated cells were incubated for 72 hours. Thereafter, the MTT reagent was introduced to a final concentration of 0.5 g/L and the plates were incubated for an additional 2 hours to allow formazan crystal formation. The supernatant was subsequently removed, and the crystals were fully dissolved by adding 140 μL of DMSO and agitating the plates for 10 minutes. The optical density of the resultant solution was quantified at a wavelength of 555 nm utilizing a microplate reader ((VICTOR X5 Multilabel Plate Reader (PerkinElmer, Waltham, MA, USA)). Data normalization and subsequent analysis, including the derivation of IC_{50} values from dose-response curves, were performed employing GraphPad Prism version 8.0.

4. Conclusions

In conclusion, this study confirms the significant antibiotic potential of oxydifficidin, a natural polyketide known to target the bacterial ribosome. We identified two producer strains, *B. velezensis* EV17 and K-3618 from distinct climate zones, and employed a toeprinting assay to demonstrate that oxydifficidin induces a generalized arrest of protein synthesis by impeding multiple stages of the translation process.

While prior research established the L7/L12 protein as a target, our findings provide a critical refinement: the binding site of oxydifficidin is distinct and does not overlap with that of the canonical translation inhibitor, thiostrepton. Furthermore, a key advantage of oxydifficidin is its selective action, as it exhibits no inhibitory effect on eukaryotic translation machinery and shows no cytotoxicity toward eukaryotic cells.

Collectively, these findings—its potent and novel mechanism of translational inhibition, coupled with its selectivity for prokaryotic systems—underscore the promise of oxydifficidin for future development. It presents a compelling candidate for applications as an effective bioprotectant against phytopathogens in agriculture and warrants further investigation for its potential therapeutic use.

Supplementary Materials: The following supporting information can be downloaded at the website of this paper posted on Preprints.org. Figure S1: Agar plates coated with *E. coli lptDmut* pDualrep2 (KanR) reporter strain and spotted with culture fluid of the producer Bacillus sp. EV17, grown on Org79 medium, and samples obtained during EV17 broth culture purification via solid-phase extraction on LPS-500-H sorbent, along with two antibiotic controls – erythromycin (Ery) (5 mg/ml) and levofloxacin (Lev) (25 mg/ml); Figure S2: HPLC of the active fraction (Gemini NX C18 150 x 10 mm, 5 μm, 110 Å; eluent solvent A - 10 mM NH4OAc, pH 5, solvent B – MeCN; isocratic elution at 40% of solvent B; flow rate 3 mL/min, UV 275 nm; Figure S3: (A) Positive-ion mode MS1 spectra of Oxydifficidin; (B) HCD mass spectra of the parentr ion [M-H]- at m/z 559.2708; Figure S4: (A) Positive-ion mode MS1 spectra of Oxydifficidin; (B) HCD mass spectra of the precursor ion at m/z 463.4219; Figure S5: Effect of oxydifficidin on translation initiation of Met-BODIPY-labeled peptide; Figure S6: Fluorescent thiostrepton derivative (Ths-FITC) and its binding to bacterial ribosomes; Table S1: The activity of enzymes and the utilization of carbohydrates by *B. velezensis* strains; Table S2: Primers and templates.

Author Contributions: Conceptualization, O.A.D., P.V.S., M.I.Z., D.A.L., S.S.T. and V.A.A; investigation, A.P.C., V.I.M., V.E.S., M.A.K., N.D.D., E.G.Y., K.A.A., E.B.G., O.A.B., S.I.K., M.N.B., A.M.K., A.E.S., M.N.R., V.K.C., M.S.G., M.E.B., V.N.T., T.V.P, M.G.K., Y.V.Z., N.V.S, A.G.T., K.S.A.; data curation, N.V.S, M.S.G.; writing—original draft preparation, A.P.C., A.G.T., M.A.K., V.I.M., Y.V.Z., E.B.G.; writing—review and editing, V.A.A., D.A.L., S.S.T., A.E.S., A.A.N., Y.V.Z., M.V.B., A.G.T.; visualization, A.P.C.; supervision, O.A.D., P.V.S., K.S.A.,

 doi:10.20944/preprints202509.1868.v1

A.A.N.; project administration, D.A.L., V.A.A., S.S.T.; funding acquisition, S.S.T., V.A.A., D.A.L., O.A.D., P.V.S. All authors have read and agreed to the published version of the manuscript.

Funding: This work was supported by the Ministry of Science and Higher Education of the Russian Federation (Agreement No. 075-15-2024-536).

Data Availability Statement: Genomic data of the strain K-3618 was taken from [20] and is available in the NCBI Assembly database under the accession number GCF_050472105.1. Genomic data of the strain EV17 is available in the NCBI Assembly database under the accession number PRJNA1320960.

Acknowledgments: We thank Center for Molecular and Cellular Biology, Genomics and Bio-imaging Core Facility for performing whole genome sequencing of genomic DNA purified from *B. velezensis* EV17 (Center for Molecular and Cellular Biology program grant for the use of shared facilities, received by I.A.V.). We are especially grateful to Dr. Ilya A. Osterman, who originally conceived this project, for supporting early aspects of this work.

Conflicts of Interest: The authors declare no conflicts of interest.

References

1. A.F. Widmer, Emerging antibiotic resistance: Why we need new antibiotics! *Swiss Med Wkly* **2022**, *152*, 40032. https://doi.org/10.57187/smw.2022.40032.
2. N.K. Boyd, C. Teng, C.R. Frei, Brief Overview of Approaches and Challenges in New Antibiotic Development: A Focus on Drug Repurposing. *Front. Cell. Infect. Microbiol.* **2021**, *11*, 684515. https://doi.org/10.3389/fcimb.2021.684515.
3. M.A. Cook, G.D. Wright, The past, present, and future of antibiotics. *Sci. Transl. Med.* 2022, 14, eabo7793. https://doi.org/10.1126/scitranslmed.abo7793.
4. S.M. Barry, Rethinking natural product discovery to unblock the antibiotic pipeline. *Future Microbiology* **2025**, *20*, 179–182. https://doi.org/10.1080/17460913.2025.2449779.
5. M.I. Hutchings, A.W. Truman, B. Wilkinson, Antibiotics: past, present and future, Current Opinion in Microbiology **2019**, *51*, 72–80. https://doi.org/10.1016/j.mib.2019.10.008.
6. T.M. Embley, E. Stackebrandt, THE MOLECULAR PHYLOGENY AND SYSTEMATICS OF THE ACTINOMYCETES, (n.d.).
7. C.T. Walsh, T.A. Wencewicz, Prospects for new antibiotics: a molecule-centered perspective, The Journal of Antibiotics **2014**, *67*, 7–22. https://doi.org/10.1038/ja.2013.49.
8. P. Zhao, Y. Xue, W. Gao, J. Li, X. Zu, D. Fu, X. Bai, Y. Zuo, Z. Hu, F. Zhang, Bacillaceae -derived peptide antibiotics since 2000. *Peptides* **2018**, *101*, 10–16. https://doi.org/10.1016/j.peptides.2017.12.018.
9. Z. Khatoon, M. del Carmen Orozco-Mosqueda, S. Huang, F.X. Nascimento, G. Santoyo, Peptide Antibiotics Produced by Bacillus Species: First Line of Attack in the Biocontrol of Plant Diseases, Bacilli in Agrobiotechnology: Plant Stress Tolerance. *Bioremediation, and Bioprospecting* 2022, 31–46. https://doi.org/10.1007/978-3-030-85465-2_2.
10. C.D. Sumi, B.W. Yang, I.-C. Yeo, Y.T. Hahm, Antimicrobial peptides of the genus *Bacillus* : a new era for antibiotics. *Can. J. Microbiol.* **2015**, *61*, 93–103. https://doi.org/10.1139/cjm-2014-0613.
11. S. Olishevska, A. Nickzad, E. Déziel, Bacillus and Paenibacillus secreted polyketides and peptides involved in controlling human and plant pathogens. *Appl Microbiol Biotechnol* **2019**, *103*, 1189–1215. https://doi.org/10.1007/s00253-018-9541-0.
12. A.F. Martinez, R.D. McMahon, M. Horner, W.M. Miller, A uniform-shear rate microfluidic bioreactor for real-time study of proplatelet formation and rapidly-released platelets. *Biotechnology Progress* **2017**, *33*, 1614–1629. https://doi.org/10.1002/btpr.2563.
13. M. Fazle Rabbee, K.-H. Baek, Antimicrobial Activities of Lipopeptides and Polyketides of Bacillus velezensis for Agricultural Applications. *Molecules* **2020**, *25*, 4973. https://doi.org/10.3390/molecules25214973.

 doi:10.20944/preprints202509.1868.v1

14. D. Saiyam, A. Dubey, M.A. Malla, A. Kumar, Lipopeptides from Bacillus: unveiling biotechnological prospects—sources, properties, and diverse applications. *Braz J Microbiol* **2024**, *55*, 281–295. https://doi.org/10.1007/s42770-023-01228-3.
15. V. Valenzuela Ruiz, A. Gándara-Ledezma, M.F. Villarreal-Delgado, E.D. Villa-Rodríguez, F.I. Parra-Cota, G. Santoyo, L.J. Gómez-Godínez, L.A. Cira Chávez, S. De Los Santos-Villalobos, Regulation, Biosynthesis, and Extraction of Bacillus-Derived Lipopeptides and Its Implications in Biological Control of Phytopathogens. *Stresses* **2024**, *4*, 107–132. https://doi.org/10.3390/stresses4010007.
16. R.O. Penha, L.P.S. Vandenberghe, C. Faulds, V.T. Soccol, C.R. Soccol, Bacillus lipopeptides as powerful pest control agents for a more sustainable and healthy agriculture: recent studies and innovations. *Planta* **2020**, *251*, 70. https://doi.org/10.1007/s00425-020-03357-7.
17. L. Wang, H. Lu, Y. Jiang, Natural Polyketides Act as Promising Antifungal Agents. *Biomolecules* **2023**, *13*, 1572. https://doi.org/10.3390/biom13111572.
18. S. Li, B. Yang, G.-Y. Tan, L.-M. Ouyang, S. Qiu, W. Wang, W. Xiang, L. Zhang, Polyketide pesticides from actinomycetes. *Current Opinion in Biotechnology* **2021**, *69*, 299–307. https://doi.org/10.1016/j.copbio.2021.05.006.
19. D.H. Parks, M. Imelfort, C.T. Skennerton, P. Hugenholtz, G.W. Tyson, CheckM: assessing the quality of microbial genomes recovered from isolates, single cells, and metagenomes. *Genome Res.* **2015**, *25*, 1043–1055. https://doi.org/10.1101/gr.186072.114.
20. E. Guglya, O. Belozerova, A. Shikov, V. Alferova, M. Romanenko, V. Chebotar, M. Gancheva, M. Baganova, E. Vinogradova, V. Lushpa, A. Baranova, M. Baranova, O. Shevtsova, A. Kudzhaev, Y. Prokopenko, D. Lukianov, K. Antonets, A. Nizhnikov, S. Terekhov, Bacillus-Based Biocontrol Agents Mediate Pathogen Killing by Biodegradable Antimicrobials from Macrolactin Family. *Preprints* **2025**. https://doi.org/10.20944/preprints202509.0481.v1.
21. L.M. Rodriguez-R, R.E. Conrad, T. Viver, D.J. Feistel, B.G. Lindner, S.N. Venter, L.H. Orellana, R. Amann, R. Rossello-Mora, K.T. Konstantinidis, An ANI gap within bacterial species that advances the definitions of intra-species units. *mBio* **2024**, *15*, e02696-23. https://doi.org/10.1128/mbio.02696-23.
22. R. Borriss, X.-H. Chen, C. Rueckert, J. Blom, A. Becker, B. Baumgarth, B. Fan, R. Pukall, P. Schumann, C. Spröer, H. Junge, J. Vater, A. Pühler, H.-P. Klenk, Relationship of Bacillus amyloliquefaciens clades associated with strains DSM 7T and FZB42T: a proposal for Bacillus amyloliquefaciens subsp. amyloliquefaciens subsp. nov. and Bacillus amyloliquefaciens subsp. plantarum subsp. nov. based on complete genome sequence comparisons. *International Journal of Systematic and Evolutionary Microbiology* **2011**, *61*, 1786–1801. https://doi.org/10.1099/ijs.0.023267-0.
23. C. Ruiz-García, V. Béjar, F. Martínez-Checa, I. Llamas, E. Quesada, Bacillus velezensis sp. nov., a surfactant-producing bacterium isolated from the river Vélez in Málaga, southern Spain. *International Journal of Systematic and Evolutionary Microbiology* **2005**, *55*, 191–195. https://doi.org/10.1099/ijs.0.63310-0.
24. Ö. Baysal, D.J. Studholme, C. Jimenez-Quiros, M. Tör, Genome sequence of the plant-growth-promoting bacterium Bacillus velezensis EU07. *Access Microbiology* **2024**, *6*. https://doi.org/10.1099/acmi.0.000762.v3.
25. M. Madhaiyan, S. Poonguzhali, S.-W. Kwon, T.-M. Sa, Bacillus methylotrophicus sp. nov., a methanol-utilizing, plant-growth-promoting bacterium isolated from rice rhizosphere soil. *International Journal of Systematic and Evolutionary Microbiology* **2010**, *60*, 2490–2495. https://doi.org/10.1099/ijs.0.015487-0.
26. V. Lefort, R. Desper, O. Gascuel, FastME 2.0: A Comprehensive, Accurate, and Fast Distance-Based Phylogeny Inference Program: Table 1. *Mol Biol Evol* **2015**, *32*, 2798–2800. https://doi.org/10.1093/molbev/msv150.
27. J.S. Farris, Estimating Phylogenetic Trees from Distance Matrices. *The American Naturalist* **1972**, *106*, 645–668. https://doi.org/10.1086/282802.
28. J.P. Meier-Kolthoff, M. Göker, TYGS is an automated high-throughput platform for state-of-the-art genome-based taxonomy. *Nat Commun* **2019**, *10*, 2182. https://doi.org/10.1038/s41467-019-10210-3.
29. I.A. Osterman, M. Wieland, T.P. Maviza, K.A. Lashkevich, D.A. Lukianov, E.S. Komarova, Y.V. Zakalyukina, R. Buschauer, D.I. Shiriaev, S.A. Leyn, J.E. Zlamal, M.V. Biryukov, D.A. Skvortsov, V.N. Tashlitsky, V.I. Polshakov, J. Cheng, Y.S. Polikanov, A.A. Bogdanov, A.L. Osterman, S.E. Dmitriev, R. Beckmann, O.A. Dontsova, D.N. Wilson, P.V. Sergiev, Tetracenomycin X inhibits translation by binding

 doi:10.20944/preprints202509.1868.v1

within the ribosomal exit tunnel. *Nat Chem Biol* **2020**, *16*, 1071–1077. https://doi.org/10.1038/s41589-020-0578-x.

30. S.B. Zimmerman, C.D. Schwartz, R.L. Monaghan, B.A. Pelak, B. Weissberger, E.C. Gilfillan, S. Mochales, S. Hernandez, S.A. Currie, E. Tejera, E.O. Stapley, Difficidin and oxydifficidin: Novel broad spectrum antibacterial antibiotics produced by Bacillus subtilis. I.Production, taxonomy and antibacterial activity. *J. Antibiot.* **1987**, *40*, 1677–1681. https://doi.org/10.7164/antibiotics.40.1677.
31. X.-H. Chen, J. Vater, J. Piel, P. Franke, R. Scholz, K. Schneider, A. Koumoutsi, G. Hitzeroth, N. Grammel, A.W. Strittmatter, G. Gottschalk, R.D. Süssmuth, R. Borriss, Structural and Functional Characterization of Three Polyketide Synthase Gene Clusters in *Bacillus amyloliquefaciens* FZB 42. *J Bacteriol* **2006**, *188*, 4024–4036. https://doi.org/10.1128/JB.00052-06.
32. M. Suphantharika, A.P. Ison, M.D. Lilly, B.C. Buckland, The influence of dissolved oxygen tension on the synthesis of the antibiotic difficidin by *bacillus subtilis*. *Biotech & Bioengineering* **1994**, *44*, 1007–1012. https://doi.org/10.1002/bit.260440818.
33. C.L.M. Gilchrist, Y.-H. Chooi, clinker & clustermap.js: automatic generation of gene cluster comparison figures. *Bioinformatics* **2021**, *37*, 2473–2475. https://doi.org/10.1093/bioinformatics/btab007.
34. I.A. Osterman, E.S. Komarova, D.I. Shiryaev, I.A. Korniltsev, I.M. Khven, D.A. Lukyanov, V.N. Tashlitsky, M.V. Serebryakova, O.V. Efremenkova, Y.A. Ivanenkov, A.A. Bogdanov, P.V. Sergiev, O.A. Dontsova, Sorting Out Antibiotics' Mechanisms of Action: a Double Fluorescent Protein Reporter for High-Throughput Screening of Ribosome and DNA Biosynthesis Inhibitors. *Antimicrob Agents Chemother* **2016**, *60*, 7481–7489. https://doi.org/10.1128/AAC.02117-16.
35. C. Orelle, S. Carlson, B. Kaushal, M.M. Almutairi, H. Liu, A. Ochabowicz, S. Quan, V.C. Pham, C.L. Squires, B.T. Murphy, A.S. Mankin, Tools for Characterizing Bacterial Protein Synthesis Inhibitors. *Antimicrob Agents Chemother* ***2013***, *57*, 5994–6004. https://doi.org/10.1128/AAC.01673-13.
36. P. Sarkar, E.A. Stringer, U. Maitra, Thiostrepton Inhibition of Initiation Factor 1 Activity in Polypeptide Chain Initiation in *Escherichia coli*. *Proc. Natl. Acad. Sci. USA* **1974**, *71*, 4986–4990. https://doi.org/10.1073/pnas.71.12.4986.
37. V.I. Marina, M. Bidzhieva, A.G. Tereshchenkov, D. Orekhov, V.E. Sagitova, N.V. Sumbatyan, V.N. Tashlitsky, A.S. Ferberg, T.P. Maviza, P. Kasatsky, O. Tolicheva, A. Paleskava, V.I. Polshakov, I.A. Osterman, O.A. Dontsova, A.L. Konevega, P.V. Sergiev, An easy tool to monitor the elemental steps of in vitro translation via gel electrophoresis of fluorescently labeled small peptides. *RNA* **2024**, *30*, 298–307. https://doi.org/10.1261/rna.079766.123.
38. J. Kan, A. Morales-Amador, Y. Hernandez, M.A. Ternei, C. Lemetre, L.W. Maclntyre, N. Biais, S.F. Brady, Oxydifficidin, a potent Neisseria gonorrhoeae antibiotic due to DedA-assisted uptake and ribosomal protein RplL sensitivity. *eLife* **2025**, *13*, RP99281. https://doi.org/10.7554/eLife.99281.
39. M.A. Carlson, B.G. Haddad, A.J. Weis, C.S. Blackwood, C.D. Shelton, M.E. Wuerth, J.D. Walter, P.C. Spiegel, Ribosomal protein L7/L12 is required for GTP ase translation factors EF -G, RF 3, and IF 2 to bind in their GTP state to 70S ribosomes. *The FEBS Journal* **2017**, *284*, 1631–1643. https://doi.org/10.1111/febs.14067.
40. M. Diaconu, U. Kothe, F. Schlünzen, N. Fischer, J.M. Harms, A.G. Tonevitsky, H. Stark, M.V. Rodnina, M.C. Wahl, Structural Basis for the Function of the Ribosomal L7/12 Stalk in Factor Binding and GTPase Activation. *Cell* **2005**, *121*, 991–1004. https://doi.org/10.1016/j.cell.2005.04.015.
41. J.M. Harms, D.N. Wilson, F. Schluenzen, S.R. Connell, T. Stachelhaus, Z. Zaborowska, C.M.T. Spahn, P. Fucini, Translational Regulation via L11: Molecular Switches on the Ribosome Turned On and Off by Thiostrepton and Micrococcin. *Molecular Cell* **2008**, *30*, 26–38. https://doi.org/10.1016/j.molcel.2008.01.009.
42. S. Schoof, S. Baumann, B. Ellinger, H. Arndt, A Fluorescent Probe for the 70 S-Ribosomal GTPase-Associated Center. *ChemBioChem* **2009**, *10*, 242–245. https://doi.org/10.1002/cbic.200800642.
43. M.F. Rabbee, Md.S. Ali, J. Choi, B.S. Hwang, S.C. Jeong, K. Baek, Bacillus velezensis: A Valuable Member of Bioactive Molecules within Plant Microbiomes. *Molecules* **2019**, *24*, 1046. https://doi.org/10.3390/molecules24061046.

 doi:10.20944/preprints202509.1868.v1

44. P. Aunkam, S. Sibponkrung, S. Limkul, T. Seabkongseng, K. Mahanil, K. Umnajkitikorn, N. Boonkerd, N. Teaumroong, S. Sato, P. Tittabutr, P. Boonchuen, Mechanisms of Cannabis Growth Promotion by Bacillus velezensis S141. *Plants* **2024**, *13*, 2971. https://doi.org/10.3390/plants13212971.
45. J.-Y. Yun, H.-S. Kim, J.-H. Moon, S.-J. Won, V. Choub, S.-I. Choi, H.B. Ajuna, P.S.-H. Lee, Y.S. Ahn, Antifungal and Plant-Growth Promotion Effects of Bacillus velezensis When Applied to Coastal to Pine (Pinus thunbergii Parl.) Seedlings. *Forests* **2023**, *15*, 62. https://doi.org/10.3390/f15010062.
46. Z. Chen, H. Zhang, W. Lv, S. Zhang, L. Du, S. Li, H. Zhang, X. Zheng, J. Zhang, T. Zhang, N. Bai, Bacillus velezensis SS-20 as a potential and efficient multifunctional agent in biocontrol, saline-alkaline tolerance, and plant-growth promotion. *Applied Soil Ecology* **2025**, *205*, 105772. https://doi.org/10.1016/j.apsoil.2024.105772.
47. L. Chen, J. Heng, S. Qin, K. Bian, A comprehensive understanding of the biocontrol potential of Bacillus velezensis LM2303 against Fusarium head blight. *PLoS ONE* **2018**, *13*, e0198560. https://doi.org/10.1371/journal.pone.0198560.
48. Y. Cao, H. Pi, P. Chandrangsu, Y. Li, Y. Wang, H. Zhou, H. Xiong, J.D. Helmann, Y. Cai, Antagonism of Two Plant-Growth Promoting Bacillus velezensis Isolates Against Ralstonia solanacearum and Fusarium oxysporum. *Scientific Reports* **2018**, *8*, 4360. https://doi.org/10.1038/s41598-018-22782-z.
49. S.M. Im, N.H. Yu, H.W. Joen, S.O. Kim, H.W. Park, A.R. Park, J.-C. Kim, Biological control of tomato bacterial wilt by oxydifficidin and difficidin-producing Bacillus methylotrophicus DR-08. *Pesticide Biochemistry and Physiology* **2020**, *163*, 130–137. https://doi.org/10.1016/j.pestbp.2019.11.007.
50. L. Wu, H. Wu, L. Chen, X. Yu, R. Borriss, X. Gao, Difficidin and bacilysin from Bacillus amyloliquefaciens FZB42 have antibacterial activity against Xanthomonas oryzae rice pathogens. *Scientific Reports* **2015**, *5*, 12975. https://doi.org/10.1038/srep12975.
51. G. Bertani, STUDIES ON LYSOGENESIS I: The Mode of Phage Liberation by Lysogenic Escherichia coli. *J Bacteriol* **1951**, *62*, 293–300. https://doi.org/10.1128/jb.62.3.293-300.1951.
52. M.G. Khrenova, T.V. Panova, V.A. Rodin, M.A. Kryakvin, D.A. Lukyanov, I.A. Osterman, M.I. Zvereva, Nanopore Sequencing for De Novo Bacterial Genome Assembly and Search for Single-Nucleotide Polymorphism. *IJMS* **2022**, *23*, 8569. https://doi.org/10.3390/ijms23158569.
53. M. Kolmogorov, D.M. Bickhart, B. Behsaz, A. Gurevich, M. Rayko, S.B. Shin, K. Kuhn, J. Yuan, E. Polevikov, T.P.L. Smith, P.A. Pevzner, metaFlye: scalable long-read metagenome assembly using repeat graphs. *Nat Methods* **2020**, *17*, 1103–1110. https://doi.org/10.1038/s41592-020-00971-x.
54. Babraham Bioinformatics - FastQC A Quality Control Tool for High Throughput Sequence Data Available online https://www.bioinformatics.babraham.ac.uk/projects/fastqc/ (accessed on 16 May 2025)., (n.d.).
55. S. Chen, Y. Zhou, Y. Chen, J. Gu, fastp: an ultra-fast all-in-one FASTQ preprocessor. *Bioinformatics* **2018**, *34*, i884–i890. https://doi.org/10.1093/bioinformatics/bty560.
56. J. Hu, J. Fan, Z. Sun, S. Liu, NextPolish: a fast and efficient genome polishing tool for long-read assembly, Bioinformatics **2020**, *36*, 2253–2255. https://doi.org/10.1093/bioinformatics/btz891.
57. J.P. Meier-Kolthoff, J.S. Carbasse, R.L. Peinado-Olarte, M. Göker, TYGS and LPSN: a database tandem for fast and reliable genome-based classification and nomenclature of prokaryotes. *Nucleic Acids Research* **2022**, *50*, D801–D807. https://doi.org/10.1093/nar/gkab902.
58. M. Richter, R. Rosselló-Móra, F. Oliver Glöckner, J. Peplies, JSpeciesWS: a web server for prokaryotic species circumscription based on pairwise genome comparison. *Bioinformatics* **2016**, *32*, 929–931. https://doi.org/10.1093/bioinformatics/btv681.
59. K. Blin, S. Shaw, L. Vader, J. Szenei, Z.L. Reitz, H.E. Augustijn, J.D.D. Cediel-Becerra, V. de Crécy-Lagard, R.A. Koetsier, S.E. Williams, P. Cruz-Morales, S. Wongwas, A.E. Segurado Luchsinger, F. Biermann, A. Korenskaia, M.M. Zdouc, D. Meijer, B.R. Terlouw, J.J.J. van der Hooft, N. Ziemert, E.J.N. Helfrich, J. Masschelein, C. Corre, M.G. Chevrette, G.P. van Wezel, M.H. Medema, T. Weber, antiSMASH 8.0: extended gene cluster detection capabilities and analyses of chemistry, enzymology, and regulation. *Nucleic Acids Research* **2025**, *53*, W32–W38. https://doi.org/10.1093/nar/gkaf334.
60. T. Baba, T. Ara, M. Hasegawa, Y. Takai, Y. Okumura, M. Baba, K.A. Datsenko, M. Tomita, B.L. Wanner, H. Mori, Construction of *Escherichia coli* K-12 in-frame, single-gene knockout mutants: the Keio collection. *Molecular Systems Biology* **2006**, *2*, 2006.0008. https://doi.org/10.1038/msb4100050.

 doi:10.20944/preprints202509.1868.v1

61. M.V. Rodnina, W. Wintermeyer, GTP consumption of elongation factor Tu during translation of heteropolymeric mRNAs. *Proc. Natl. Acad. Sci. USA* **1995**, *92*, 1945–1949. https://doi.org/10.1073/pnas.92.6.1945.
62. Z.-X. Wang, An exact mathematical expression for describing competitive binding of two different ligands to a protein molecule. *FEBS Letters* **1995**, *360*, 111–114. https://doi.org/10.1016/0014-5793(95)00062-E.
63. T. Mosmann, Rapid colorimetric assay for cellular growth and survival: Application to proliferation and cytotoxicity assays. *Journal of Immunological Methods* **1983**, *65*, 55–63. https://doi.org/10.1016/0022-1759(83)90303-4.